International Journal of Rock Mechanics and Mining Sciences 104 (2018) 100–112

Contents lists available at ScienceDirect

International Journal of Rock Mechanics and Mining Sciences

journal homepage: www.elsevier.com/locate/ijrmms

Experimental investigation of the anisotropic mechanical behavior of phyllite under triaxial compression

Guowen Xu*, Chuan He, Ang Su, Ziquan Chen

Key Laboratory of Transportation Tunnel Engineering, Ministry of Education, Southwest Jiaotong University, Chengdu 610031, Sichuan, China

ARTICLE INFO

Keywords:
Anisotropy
Triaxial compression
Scanning electron microscope (SEM)
Acoustic emissions(AE)
Fractal property

1. Introduction

The physical and mechanical properties (e.g., strength, permeability, and heat transfer) of anisotropic rocks are affected significantly by weak planes (i.e., the bedding plane, foliation, stratification, layering, fissuring, and jointing).[1,2] Numerous engineering projects have dealt with anisotropic rocks, including underground excavation,[3,4] the storage of radioactive materials,[5,6] and oil and gas exploration.[7] In recent years, the behavior of anisotropic rocks, including phyllite,[8,9] schist,[10–14] gneiss,[12,13] slate,[15] shale,[13,16–18] sandstone,[19–21] and synthetic rock,[22] has been attracting increased interest, and their behavior has been studied using uniaxial and triaxial compression tests. The experimental results indicated that there were three universal phenomena, i.e., (1) types for which compressive strength varies as a function of θ (the angle between the loading direction and the weak planes) can be divided into U-type, undulatory-type, and shoulder-type[23]; (2) the maximum strength occurred at θ = 0° or 90°, while the minimum strength occurred between θ = 30° and 45°, and the degree of anisotropy represented in terms of the compressive strength decreases as the confining pressure increased; (3) there were four kinds of macro-fracture patterns, i.e. tensile splitting along or across weak planes, sliding failure along weak planes, and composite shear failure across and along weak planes.

The aforementioned experiments provided information concerning the significance of weak planes on the strength and macro-fracture patterns of anisotropic rocks and placed less emphasis on the anisotropy of the fracture mechanism at the mesoscopic level. Various test technologies, e.g., CT, SEM, and AE, are used extensively in the study of the meso-mechanical behavior of isotropic rocks.[24–28] However, there are still few experimental results for anisotropic rocks. Louis et al.[29] used X-ray CT and SEM to examine the fracture mechanism of sandstone with a layered structure. Kim et al.[30] developed a numerical approach based on the results of CT scans to simulate the anisotropic feature of Berea sandstone. Ambrose[31] obtained CT scan images of the fracture planes of Bossier shale with different confining pressures and foliation-loading angles during triaxial compression tests. Debecker and Vervoort[32] recorded AE events during uniaxial compression tests of slate to analyze the damage process.

The results of these past research projects clearly indicate that weak planes affect the macroscopic fracture patterns, the mesoscopic failure mechanisms, and the failure process of anisotropic rock. A comprehensive study of these phenomena will help gain a better understanding of the anisotropic features of rock. Thus, this paper describes our use of triaxial compression tests to investigate the anisotropy of phyllite with different water contents. In addition to fracture patterns and strength, the mesoscopic failure mechanisms were obtained through SEM fractographic studies and 3D laser profilometry on the fractured surface. In addition, the initiation and propagation processes of micro-cracks were analyzed systematically using the temporal and spatial distributions of the AE counts.

2. Preparation of experiment

2.1. Preparation of specimens

Phyllite specimens were obtained from the Zhegu mountain tunnel, which is located on the highway from Wenchuan County to Barkam City in Sichuan Province, China. The tunnel has two lanes for traffic in

* Corresponding author.
E-mail address: xgw80033@163.com (G. Xu).

https://doi.org/10.1016/j.ijrmms.2018.02.017
Received 31 March 2017; Received in revised form 11 December 2017; Accepted 5 February 2018

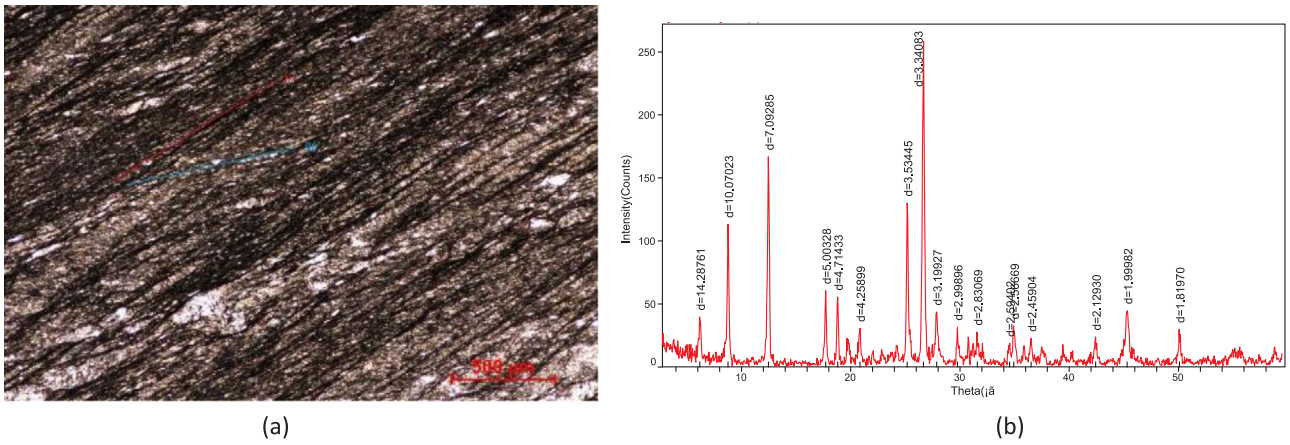

Fig. 1. Experimental results of rock sample: (a) Single-polarized micrographs; (b) X-ray diffraction.

one direction, and these two lanes are separated from the other two lanes for traffic in the opposite direction. The length of the tunnel is 8784 m, its width is 13.4 m, its height is 10.5 m, and its maximum buried depth is about 1300 m.

The single polarized micrograph of a thin section (Fig. 1a) shows that the sample was dark gray with a blastopelitic texture and a weak tabular structure. X-ray diffraction analysis of the powdered rock (Fig. 1b) indicated that the main minerals were illite, chlorite, quartz, and plagioclase, which accounted for 40%, 33%, 19%, and 8% of the total mass respectively.

The original size of the phyllite block approximately 300 × 300 × 300 mm, and the angles between the foliation and the drilling direction were 0°, 30°, and 90°. During the preparation of the specimens, it was found that specimens were much easier to get at $\theta = 0°$ than at $\theta = 30°$ or 90°. As indicated in Table 1, 15 cylindrical specimens with diameters of 50 mm and lengths of 100 mm were prepared for the triaxial compression tests.

2.2. Experimental process

The triaxial compression tests were conducted using a rock mechanics test system (Model MTS 815). A system for monitoring AE signals, manufactured by the American Physical Acoustic Corporation, was used during the experiment. The AE sensors were Mic 30 sensors that had a resonant frequency of 200 kHz and a recording frequency that ranged from 20 kHz to 1 MHz. The sampling frequency was 1 MHz, and the threshold amplitude was 40 dB. Eight probes were arranged on the outside of the chamber and used to locate the AE events. The loading process was done as follows according to the method suggested by ISRM[33]:

(1) First, the confining pressure and the axial pressure were applied simultaneously at a loading rate of 6 MPa/min until the confining pressure reached the required value.

(2) Then, the confining pressure was kept constant, and the axial load was increased at a loading rate of 60 kN/min, and the axial and circumferential strains on the specimen were recorded. When the load reached 80% of the peak load, the loading control mode was changed from axial pressure control to circumferential strain control with a rate of 0.02 mm/min until the specimen failed.

3. Experimental results

3.1. Stress-strain curve

Fig. 2 shows the stress-strain curves of the specimens for different cases. The figure shows that, as the confining pressure was increased, specimens with the same water content and foliation-loading angle had increased axial strains that corresponded to the peak compressive strength. In all cases, the specimens underwent brittle failure, indicating that the confining pressure did not reach the conversion magnitude that prompts the failure pattern to be transformed from brittle failure to ductile failure.

Fig. 2a-c show the stress-strain curves of specimens with natural water content. For $\theta = 90°$, the post-peak behavior is type I (the slope

Table 1
Mechanical parameters of specimens.

specimen	σ_3(MPa)	σ_c/MPa	σ_{ci}(MPa)	σ_{cD}(MPa)	σ_{ci}/σ_c	σ_{cD}/σ_c	E_s/GPa	$\varepsilon_1/10^{-3}$	$\varepsilon_3/10^{-3}$	$\varepsilon_v/10^{-3}$
90-n-10	10	142.63	68.5	115.4	48.0%	80.9%	30.34	5.75	−1.26	3.23
90-n-20	20	174.41	85.4	134.5	49.0%	77.1%	35.91	6.44	−1.86	2.71
90-n-30	30	198.69	102.2	156.3	51.4%	78.7%	43.37	6.38	−1.86	2.64
30-n-10	10	96.8	38.1	76.5	39.4%	79.0%	36.32	3.71	−0.91	1.89
30-n-20	20	122.86	52.3	93.2	42.6%	75.9%	43.84	4.29	−0.93	2.43
30-n-30	30	151.93	67.4	102.7	44.4%	67.6%	48.31	4.15	−0.77	2.59
0-n-10	10	128.8	43.2	85.4	33.5%	66.3%	39.95	4.11	−0.92	2.27
0-n-20	20	159.87	66.2	138.5	41.4%	86.6%	47.13	4.23	−1.84	0.56
0-n-30	30	190.90	79.3	163.2	41.5%	85.5%	55.15	4.13	−2.61	−1.09
0-d-10	10	143.32	33.4	92.1	23.3%	64.3%	49.23	3.56	−0.77	2.01
0-d-20	20	175.37	65.3	132.5	37.2%	75.6%	58.01	3.94	−0.95	2.03
0-d-30	30	220.95	84.7	173.2	38.3%	78.4%	86.89	9.1	−4.77	−0.44
0-s-10	10	65.3	22.1	43.2	33.8%	66.2%	32.75	2.64	−0.58	1.49
0-s-20	20	78.04	30.9	63.2	39.6%	81.0%	40.47	2.81	−1.61	−0.41
0-s-30	30	110.74	44.2	85.4	39.9%	77.1%	50.56	3.26	−1.59	0.06

Note: the name of specimen is composed of three items, representing foliation-loading angel θ, water content (n is natural and the content is 4.5%, d is dry and s is saturated) and confining pressure in sequential order.